Soft Matter

Accepted Manuscript

This article can be cited before page numbers have been issued, to do this please use: N. A. Pérez Chávez, V. Nosthas Aguiar, J. A. Allegretto, A. Albesa, J. M. Giussi and G. S. Longo, *Soft Matter*, 2020, DOI: 10.1039/D0SM00951B.

ROYAL SOCIETY OF CHEMISTRY

rsc.li/soft-matter-journal

View Article Online
DOI: 10.1039/D0SM00951B

Soft Matter

ARTICLE TYPE

Cite this: DOI: 00.0000/xxxxxxxxxx

Triggering Doxorubicin Release from Responsive Hydrogel Films by Polyamine Uptake†

Nestor A. Pérez-Chávez,[a] Victor Nosthas Aguiar,[a] Juan A. Allegretto,[a,b] Alberto G. Albesa,[a] Juan M. Giussi,[a] and Gabriel S. Longo*[a]

Received Date
Accepted Date

DOI: 00.0000/xxxxxxxxxx

Polyamines such as putrescine, spermidine and spermine are required in many inter- and intra-cellular processes. There is, however, evidence of anomalously high concentrations of these polyamines around cancer cells. Furthermore, high polyamine concentrations play a key role in accelerating the speed of cancer proliferation. Some current therapies target the reduction of polyamine concentration to delay cancer advance. In this study, we use a molecular theory to proof the concept that poly(methacrylic acid) (PMAA) hydrogels can play the dual role of incorporating and retaining polyamines as well as releasing preloaded drugs in response. To such goal, we have developed a molecular model for each of the chemical species, which includes the shape, size, charge, protonation state, and configuration. Our results indicate that PMAA hydrogel films can incorporate significant amounts of polyamines; this absorption increases with the solution concentration of polyamines. Doxorubicin was chosen as a model drug for this study, which can be successfully incorporated within the film; the optimal encapsulation conditions occur at low salt concentrations and pH values near neutrality. Polyamine absorption within the film results in the desorption of the drug from the hydrogel. An increasing concentration of polyamines enhances drug release. To validate our theoretical findings, poly(methacrylic acid) hydrogel thin films were synthesized by Atom Transfer Radical Polymerization. Absorption/desorption experiments followed by UV-Vis spectroscopy demonstrate doxorubicin encapsulation within these films and polyamine dependent drug release.

1 Introduction

Putrescine, spermidine and spermine are polyamines having two, three and four amino groups, respectively, which are present in all living cells. Polyamines are indispensable to cell growth and required in many intra/inter-cellular processes. They participate in diverse metabolic functions such as DNA replication, ion channels regulation, protein phosphorylation, and extracellular signalling[1,2]. Moreover, polyamines interact strongly with membrane phospholipids, and may thus play an important role in the regulation of membrane-linked enzymes[3]. The synthesis of these essential molecules begins when the enzyme ornithine decarboxylase (ODC) catalyzes the production of putrescine[2,4,5].

In the surroundings of healthy cells, polyamines are found in high micromolar to low millimolar concentrations[6,7]. Near tumor cells, however, their concentration is relatively higher. Many studies have shown that cancer patients have increased polyamine concentrations both in blood and urine[8], which results from the higher activity of ODC[2,9,10]. Anomalous polyamine concentrations can mark the presence of a tumor cell[11,12], but also an excess polyamine availability can increase the speed at which tumors spread and metastasize[2]. At the same time, such excess can inhibit immune mechanisms that cell have in place to prevent tumor spreading[2,13]. Indeed, patients with increased levels of polyamine generally receive poorer prognosis[2,14]. There is currently great interest in cancer therapies that can regulate/reduce the amount of polyamines in the vicinity of tumor cells to prevent their spreading[2,15–17]. In this work, we propose and explore both theoretically and experimentally the concept of a functional biomaterial capable of absorbing polyamines but at the same time using the excess concentration of these markers near tumor cells as a trigger for the release of a therapeutic drug.

Hydrogels of cross-linked polymer chains are currently considered for diverse applications to biomedical research[18]. For example, biomaterials based on pH-sensitive hydrogels have been explored as oral drug delivery vehicles that have the potential to encapsulate and transport a therapeutic agent through the gastrointestinal tract, protecting the cargo from the acidic medium of the stomach, and release it at the neutral environment of the small intestines[19–22]. These hydrogels are responsive to pH changes

[a] Instituto de Investigaciones Fisicoquímicas, Teóricas y Aplicadas (INIFTA), UNLP-CONICET, La Plata, Argentina; * E-mail: longogs@inifta.unlp.edu.ar
[b] Universidad Nacional de San Martín (UNSAM), San Martín, Argentina.

† Electronic Supplementary Information (ESI) available: Additional Results. See DOI: 10.1039/cXCP00000x/

View Article Online
DOI: 10.1039/D0SM00951B

because they contain a significant number of weak acidic groups. Here, we will consider a poly(methacrylic acid) (MAA) hydrogel film. Hydrogels of PMAA are capable of responding to diverse biological stimuli, including changes in the physiological pH[23]. In this context, our present contribution addresses a fundamental question: Is it possible to exploit the environment sensitive properties of weak polyacid hydrogels in developing a biomaterial that can simultaneously incorporate/sequester polyamines and release a therapeutic drug in response?

Doxorubicin is an anthracycline that is commonly used in chemotherapy due to its efficacy in fighting a wide range of cancers such as carcinomas, sarcomas and hematological cancers[24]. It is one of the most potent antineoplastic drugs with the experimental advantage that it can be monitored by fluorescence and/or absorbance[25]. Used alone or in combination with other therapeutic agents, Doxorubicin is currently the compound of its class having the widest spectrum of activity[26]. In addition, because it is positively charged, doxorubicin can be encapsulated within anionic nanogels[22] or immobilized at the surface of negatively charged nanohydrid surfaces[27].

The aim of this study is to characterize PMAA hydrogels as materials that can capture polyamines and simultaneously release doxorubicin in response. To this goal, we apply a recently developed molecular theory to investigate the absorption from polyamines and doxorubicin solutions to PMAA hydrogel films. This theory is formulated on the basis of a general thermodynamic potential that accounts for the free energy cost of protonation/deprotonation of titratable units, the entropic loss of molecular confinement, the conformational and translational degrees of freedom of both the polymer layer and the absorbates, and the electrostatic and steric interactions. Our molecular model includes size, shape, configuration, and local charge-state description of all chemical species present in the system (spermidine, spermine, putrescine, doxorubicin and the PMAA network).

Finally, PMAA films were synthesized, and by choosing a set of representative conditions from the entire theoretically-explored collection, we have performed polyamines and doxorubicin absorption experiments followed by UV-Vis technique. These experiments demonstrate the suitability of the present approach to explore new biomaterials and its response in the context of cancer applications. In summary, here we explore the physicochemical behavior of the hydrogels from a theoretical perspective, which allows for a systematic study of its response to changes in pH, salt and polyamine concentration, and also from an experimental perspective, to prove the key points found by our calculations.

2 Methods

2.1 Theoretical Approach

2.1.1 Theory

The system that we study is schematized in Fig. 1. A surface-grafted cross-linked poly(methacrylic acid) network is in equilibrium with a solution containing water molecules, hydronium and hydroxide ions, and sodium chloride, which is completely dissociated into chloride and sodium ions. In addition, this solution contains either doxorubicin or a polyamine or both species. The

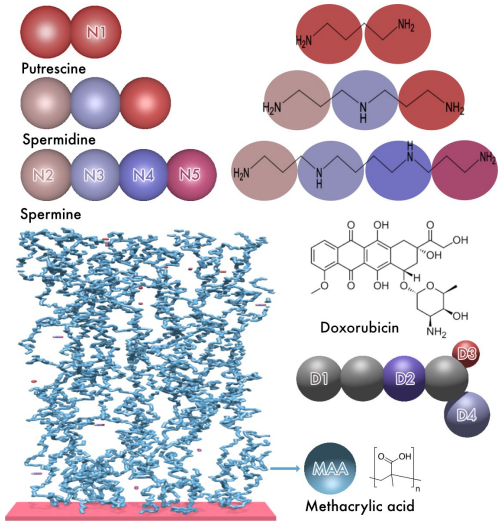

Fig. 1 The scheme presents the system of study and illustrates the coarse grain model employed to describe the different chemical species. A surface-grafted cross-linked PMMA network is in contact with an aqueous solution that can contain doxorubicin and/or one of the polyamines.

polyamines we have considered are putrescine, spermidine and spermine.

To study this system we apply a molecular theory that was recently developed to investigate absorption to such pH-responsive hydrogel films from protein mixtures[28,29]. Our approach is based on the work of Szleifer and collaborators to study the behavior of grafted weak polyelectrolyte layers[30,31]. The method here employed is general and flexible; it has for example been applied for the study of glyphosate sequestration in poly(allyl amine) hydrogels[32].

Next, we will present a concise description of the theory with emphasis in the molecular model introduced to describe doxorubicin, putrescine, spermidine and spermine. A full description of this molecular model can be found in our previous work[28].

The first step is the formulation of a general free energy including all the relevant contributions:

$$\begin{aligned} F = & -TS_{conf,nw} + F_{chm,nw} - TS_{mix} \\ & + \sum_i \left(-TS_{tr,i} - TS_{conf,i} + F_{chm,i}\right) \\ & + U_{ste} + U_{elec} \end{aligned} \tag{1}$$

where T is the system temperature, and $S_{conf,nw}$ is the network's configurational entropy; this contribution results from the different molecular conformations that the cross-linked polymer can assume. The chemical free energy that describes the protonation equilibrium of titratable units of the network is $F_{chm,nw}$. The mixing entropy of the small mobile species is S_{mix}, which describes the translations of water molecules, hydronium, hydroxide and salt ions.

The sum in the second line of Eq. (1) considers the free energy contributions from the absorbates. The subindex i runs over the absorbates in the solution: doxorubicin and/or putrescine, spermidine and spermine (we consider solutions having either the

View Article Online
DOI: 10.1039/D0SM00951B

drug or a polyamine as well as solutions having both). For each of these species, $S_{tr,i}$ and $S_{conf,i}$ are its translational and configurational entropy, while $F_{chm,i}$ is the chemical free energy of its protonable units. The energetic contributions to the free energy include steric repulsions (at the excluded-volume level), U_{ste}, and the electrostatic interactions, U_{elec}.

Each of these contributions to the free energy can be written as a functional of a few functions: (i) the probability distribution of network conformations, (ii) the local (position dependent) densities of all mobile species, (iii) the local degree of charge of all titratable units, including those of the polymer network and those of the absorbates, and (iv) the local electrostatic potential.

The free energy functional is then minimized with respect to each functions (i)-(iv). In performing this step, we consider that the proper thermodynamic potential whose minimum yields the equilibrium conditions is the semigrand potential, which is a function of the chemical potentials of the free species.

This procedure allows for expressing functions (i)-(iii) in terms of two unknown local potentials: the osmotic pressure and the electrostatic potential. These potentials can be obtained solving the solution incompressibility constraint and the Poisson equation.

To solve these equations we use some approximations: a homogeneous system in the plane of the surface that supports the film ($x-y$ plane) is considered. Changes occur along the normal direction to that plane, where z is the coordinate that measure the distance from the supporting surface. While the grafting surface sits at $z=0$, $z\to\infty$ corresponds to the bulk solution, which is homogeneous. The solutions to the system of non-linear coupled differential equations that result from minimizing the free energy are obtained numerically using a Newton-Krylov method with a space discretization of 0.5 nm along the z-direction.

2.1.2 Molecular Model

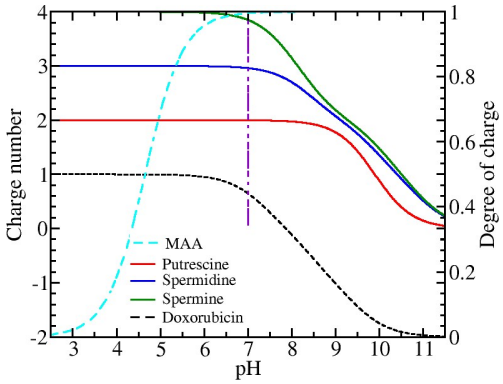

Fig. 2 Average net charge number of doxorubicin and the polyamines as a function of pH in dilute solutions. The right-hand side axis gives the degree of charge of an isolated methacrylic acid unit. The vertical dash-dotted line indicates physiological pH. (Theoretical predictions.)

Our theoretical formalism requires a molecular representation of all chemical species in the system. Figure 1 includes the coarse grain scheme used for MAA and the species in solution. Polyamines (putrescine, spermidine and spermine) are represented using their different amine groups (N1 to N5). Doxorubicin model includes the rings (D1, D2 and D4) as well as the carboxylic group (D3). The volume, pKa and charge of these groups, and those of water molecules and ions, are presented in Table 1. The molecular geometries as well as the pKa values assigned to the different coarse grain units have all been obtained from the literature[9,33,34].

The polymer network is made of 50-segment long cross-linked chains; each chain segment is a coarse grain representation of a MAA unit (see Fig. 1). This network has diamond-like topology with the cross-linking units having coordination four[35–38]. Network conformations are generated using Molecular Dynamics simulations as described in Hagemann *et al.* [28].

With the above described pKa scheme, Fig. 2 shows the average electric charge of each polyamine and that of doxorubicin. The graph also displays the degree of charge of an isolated MAA monomer in dilute solution. The driving force for absorption are the absorbate-MAA electrostatic attractions. The positive charge of all the absorbates decreases with increasing pH. The polymer becomes more negatively charged with increasing pH. Then, we expect absorption to be a nonmonotonic function of the solution pH. In addition, the isoelectric point of doxorubicin is around neutral pH, which implies that the drug is charge neutral at physiological conditions and negatively charged at higher pH values. In Section 3, we will discuss the role of doxorubicin charge regulation in its absorption/desorption in/from the hydrogel.

CG unit	pKa	q	v (nm^3)
N_1	9.9	(+1)	0.051
N_2	10.9	(+1)	0.051
N_3	8.4	(+1)	0.063
N_4	7.9	(+1)	0.063
N_5	10.1	(+1)	0.051
D_1	-	0	0.085
D_2	7.34	(-1)	0.085
D_3	8.46	(-1)	0.035
D_4	9.46	(+1)	0.085
MAA	4.65	(-1)	0.065
H_2O	-	0	0.03
H_3O^+	-	+1	0.03
OH^-	-	-1	0.03
Na^+	-	+1	0.033
Cl^-	-	-1	0.033

Table 1 Coarse grain model. The pKa values assigned to the different coarse grain units have all been obtained from the literature[9,33,34], and the molecular volumes correspond to Van der Waals values. () indicate the charge of the ionized chemical species.

2.2 Experiments

In order to support the theory and molecular modelling, cross-linked polymeric films based on poly(methacrylic acid) have been prepared and experiments of doxorubicin loading and release in presence of spermine and spermidine have been carried out. Contact angle of the film at each step was measured to follow the synthetic procedure.

View Article Online
DOI: 10.1039/D0SM00951B

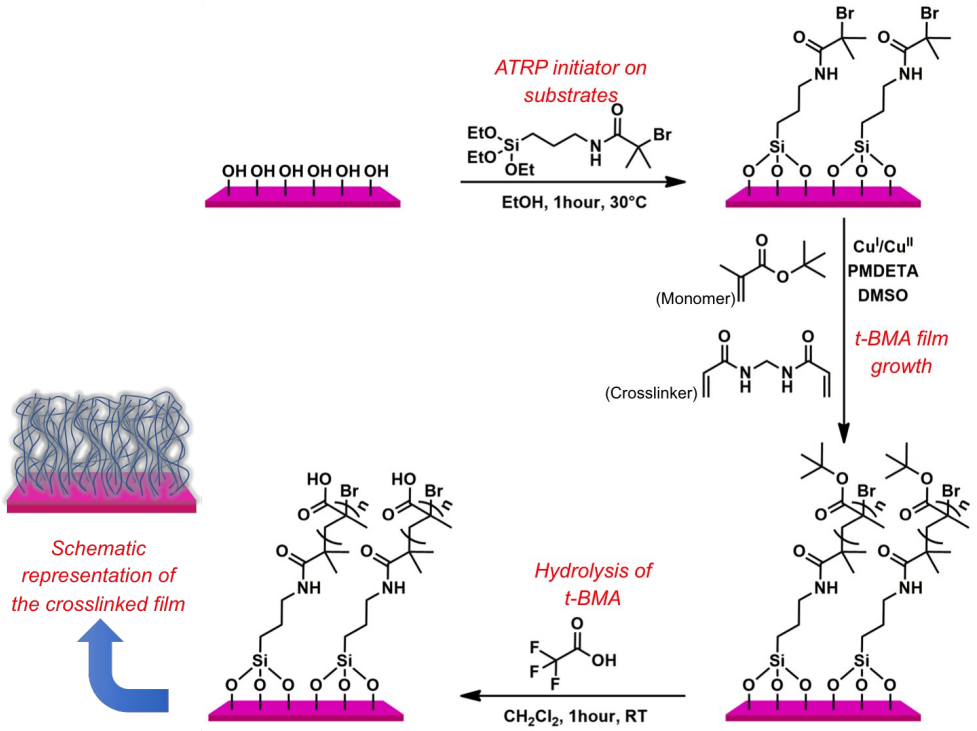

Fig. 3 Steps of the thin PMAA film synthesis, represented as: A) ATRP initiator on substrates; B) t-BMA film growth; C) hydrolysis of t-BMA. Contact angle measurements can be found in the ESI, which confirm successful substrate modification after each step.

2.2.1 Controlled growth of PMAA thin film

Thin PMAA films were obtained by Atom Transfer Radical Polymerization (ATRP) technique, which allows the surface-initiated polymerization. The complete PMAA film synthesis requires three main steps as represented in Fig. 3. These steps are: 1) grafting of ATRP initiator on substrates (Glass coverslips and single-polished silicon wafers); 2) ATRP procedure using ter-butyl methacrylate (t-BMA) and N,N'-Methylenebisacrylamide (BIS) as the cross-linker; and 3) hydrolysis of the resulting cross-linked ter-butyl methacrylate films with trifluoroacetic acid to obtain the PMAA films.

1) ATRP initiator on substrates. After cleaning with soapy water, ethanol and acetone in a ultrasonic bath, glass coverslips and silicon wafers were modified by immersion in a solution 2% v/v of 2-bromo-2-methyl-N-(3-(triethoxysilyl)propyl) propenamide (prepared as previously reported[39]) in dry ethanol for 1 hour at 30°C. The substrates were then washed with ethanol and cured for 2 h in an oven at 60°C under vacuum. The measured contact angle (Ramè-Hart Contact Angle goniometer model 290) using water was around $63.6° \pm 0.1°$ without changes over time, slightly lower than for the glass slide ($64.7° \pm 0.2°$). The full set of measurements is shown in the Electronic Supplementary Information (ESI).

2) Ter-butyl methacrylate film growth. The ATRP polymerizations were carried out according to Brown *et al.*[40]. A solution of t-BMA (15 ml, 92 mmol, Aldrich 98%), BIS (422 mg, 2.76 mmol, Aldrich 99%), $CuBr_2$ (4.1 mg, 0.018 mmol, Aldrich 99.999%), and N,N,N,N,N-Pentamethyldiethylenetriamine (PMDETA, 0.12 ml, 0.55 mmol, Aldrich, 99%) dissolved in DMSO (15 ml) was degassed by N_2 bubbling for an hour at room temperature. Then, CuBr (26.5 mg, 0.18 mmol, Aldrich 99.999%) was added and the mixture was left under N_2 for 15 min. Simultaneously, initiator substrates were sealed in Schlenk tubes and degassed through vacuum/N_2 cycles. Then, the reaction mixture was syringed into these Schlenk tubes to cover completely the samples. The mixture was left 24 h under N_2 and the substrates were then removed and washed with DMSO, acetone and dried with N_2. The measured contact angle was $89.3° \pm 0.1°$ without changes over time.

3) Hydrolysis of obtained cross-linked ter-butyl methacrylate. Cross-linked PtBMA films were immersed in a solution of Trifluoroacetic Acid (Aldrich 99%) in CH_2Cl_2 (50% v/v) for one hour at room temperature. The substrates were then washed with water several times and were left immersed in water 10 minutes and dried with N_2. The measured contact angle using water decreased over time, from an initial value around of 69° to 63°; this behavior indicates a successful hydrolysis of the PtBMA film into a more hydrophilic PMAA film, exposing carboxylic moieties, which is swelling/hydrating over time.

2.2.2 Doxorubicin loading and release in presence of polyamines

The doxorubicin (Doxo, Aldrich 98.0-102.0% in doxorubicin hydrochloride) loading was performed immersing the PMAA films in a 10^{-2} M solution of the drug in ultrapure *Milli-Q* water (18.2 MΩ cm) during 24 h in the fridge (see Fig. 4). Using a UV-Vis Lambda 35, Perkin Elmer spectrometer, the absorption bands of Doxo in the $450 - 550$ nm were used to characterize its loading in the film. To such end, after loading, the substrates were immersed for a few seconds in ultra pure water to remove surface-attached

View Article Online
DOI: 10.1039/D0SM00951B

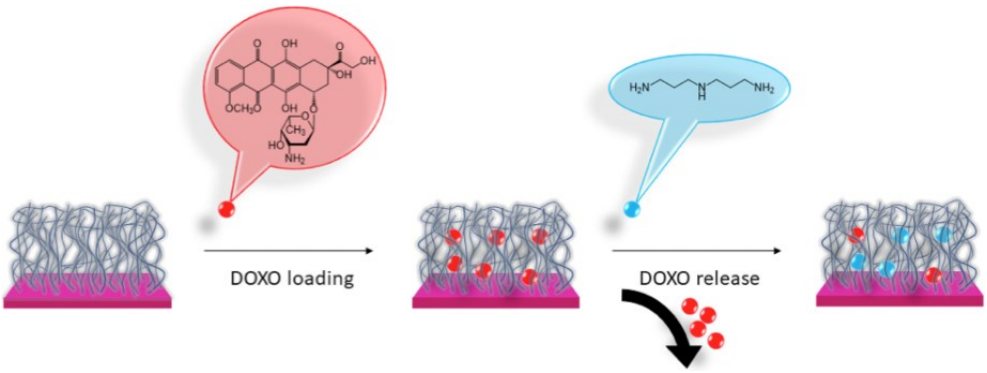

Fig. 4 Scheme showing doxorubicin loading to the PMAA hydrogel film and release in presence of spermidine**.

molecules and dried under a N_2 stream. Finally, the substrates were placed vertically in the optical path of the spectrometer and the scans were performed, covering the 200-800 nm range, with a 480 nm/min scan rate and a slide width of 1 nm.

The release was performed by immersing the loaded substrates either in water or in solutions of spermidine (Aldrich $> 99\%$) or spermine (Aldrich $> 97\%$), each at 2.8% w/v (see Fig. 4) at different times. The release was followed in the same way as the loading. These polyamine solutions were neutralized with sodium hydroxide 0.1 M, which increased the ionic strength from pure water and lead to a final pH of 7. All the experiments were performed using ultrapure *Milli-Q* water. Polyamine concentration was chosen in order to explore a saturation regime, equivalent to the extreme of the explored region in the theoretical predictions (see below). In this way, equivalent amine loading quantities can be qualitatively compared.

3 Results and Discussion

3.1 Theoretical Results

The first question that we address is how PMAA hydrogels respond to polyamine solutions. Our thermodynamic approach allows for considering the absorption inside the polymer network from solutions containing these amines. We define the absorption as

$$\Gamma_i = \int_0^\infty (\rho_i(z) - \rho_i^{bulk}) dz \qquad (2)$$

where the coordinate z measures the distance from the surface that supports the film, and the subindex i refers to the absorbate of interest. The local function $\rho_i(z)$ is the density of the absorbate, and $\rho_i^{bulk} = \lim_{z\to\infty} \rho_i(z)$ is that of the bulk solution, far from the hydrogel film. This definition of Γ quantifies the mass of absorbed molecules per unit area in excess of the contribution imposed by the bulk solution. The expression given by Eq. (2) describes the absorption of each of the amines, but it is also valid for doxorubicin.

Figure 5 shows absorption isotherms for each of the polyamines as a function of its concentration in the bulk solution. Because there are reports that the surroundings of tumor cells are acidic[41–46], we include absorption isotherms for different pH values. We emphasize that our fist objective is to investigate the capacity of PMAA hydrogels to sequester polyamines at physiological conditions; then, the results of Fig. 5 correspond to solutions without doxorubicin and 100 mM of $[NaCl]$. As expected, absorption increases with increasing concentration of polyamines. This is an indication of a non-saturated regime being achieved with the explored concentration, which is easily seen from the absorption isotherms.

Further on, near healthy cells, polyamine concentration is in the range from 10^{-4} to 10^{-3} M, which can increase one order of magnitude or more around tumors[2]. The results of Fig. 5 suggest that PMAA hydrogels can respond to these conditions by capturing increasing amine quantities. In particular, putrescine displays a seemingly on/off behavior around the onset of the healthy to pathological concentrations. In addition, except for the most acidic solutions (pH 5), this absorption behavior holds for different pH values around physiological conditions, which points to the hydrogel's ability to adapt to small pH changes caused by damaged cells.

Absorbed polyamines are distributed more or less homogeneously within the hydrogel film (see ESI). Such distribution however is correlated with the polymer density: higher concentrations of polyamine are found in the regions of locally high volume fraction of PMAA (see ESI). Therefore, polyamines have a higher probability of being found near network cross-links, which is where the highest polymer density occurs. Similar behavior has been predicted by Sai *et al.*[47] using molecular dynamics simulations, who suggested that chromophore amphiphiles self-assembly at the nodes of chemically cross-liked polyelectrolyte hydrogels.

Under similar conditions, the hydrogel absorbs more spermine than spermidine and putrescine (compare panels A, B and C of Figure 5, respectively), which can be explained on the basis of the net positive charge of the polyamines: the more charged the amine is, the more it absorbs to the film because a higher positive charge reduces the entropic cost of counterion confinement while allowing for the electrostatic attractions with the MAA polymer.

Schimka *et al.*[48] have studied the interaction between polymer microgels and light-sensitive surfactants with synthetic polyamines as head groups. These surfactants have different

** This scheme does not describe the swelling behavior of the hydrogel film.

View Article Online
DOI: 10.1039/D0SM00951B

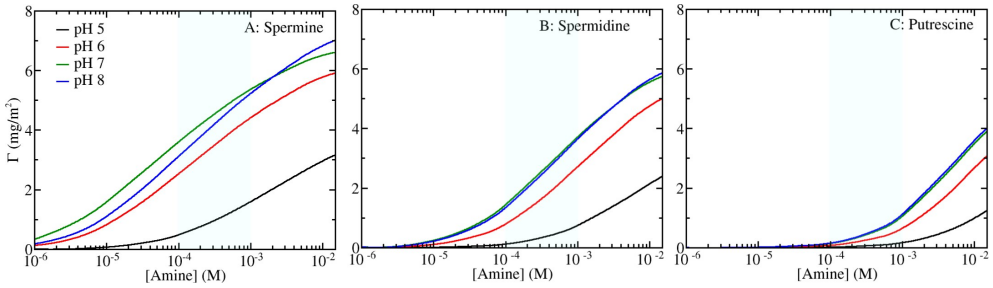

Fig. 5 Plot of the absorption, Γ, of spermine (A), spermidine (B) and putrescine (C) as a function of its (bulk) solution concentration. The various curves in each panel correspond to different pH values (around 7) and physiological salt conditions, $[NaCl] = 100\,\text{mM}$. Shaded regions indicate the range of healthy polyamine concentrations[2]. There is no doxorubicin in these solutions. (Theoretical predictions.)

numbers of amino groups with charges between +1 and +3. The anionic microgels deswell when exposed to a sufficiently high concentration of surfactant (depending on the isomerization state of the surfactant). Their study shows both experimentally and theoretically that a larger concentration of surfactant is needed to trigger microgel deswelling when decreasing the charge of the polyamine head group. Such behavior indicates that increasing the number of amino groups facilitates surfactant uptake by the microgel, in agreement with our results.

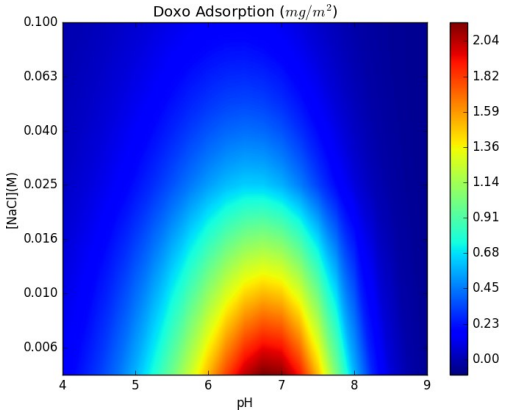

Fig. 6 Color map showing the absorption of doxorubicin (see Eq. (2)) as function of the composition of the solution that embeds the hydrogel, *i.e.*, pH and $[NaCl]$; the concentration of the drug in the solution is $[Doxo] = 1\,\text{mM}$. (Theoretical predictions.)

Next, we consider the ability of PMAA hydrogel films to incorporate doxorubicin (Doxo). Hydrogels of cross-linked polyacid chains are sensitive to changes in solution ionic strength or salt concentration[49]. This behavior may be not be relevant in biological environments with highly regulated concentration of ions, but controlling salt concentration is critical in the lab to enhance loading the therapeutic agent inside the material. Then, we have considered doxorubicin absorption for typical lab conditions, covering a wide range of pH and $[NaCl]$, as opposed to physiological conditions.

Figure 6 shows the excess absorption of Doxo, calculated using Eq. (2). This graph highlights the effect of decreasing salinity to boost drug absorption. Because doxorubicin charge is +1 (at low pH), its absorption competes with that of sodium ions to neutralize the charge of the polymer. Therefore, the best conditions for its incorporation into the film correspond to reducing the availability of salt counterions.

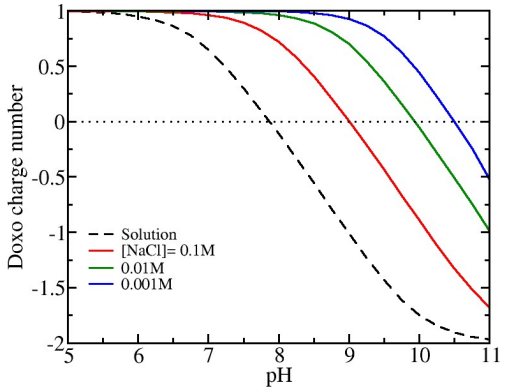

Fig. 7 Plot showing doxorubicin charge number inside the PMAA network as a function of pH, for different salt concentrations (solid lines) as well as the average charge of the molecule in the bulk solution (dashed line); $[Doxo] = 1\,\text{mM}$. (Theoretical predictions.)

In our model doxorubicin has its isoelectric point (pI) at pH 7.8. Interestingly, Fig. 6 shows that the optimal conditions for the electrostatically-driven absorption occurs at pH values near pI. This result can be explained considering that pH drops inside the film (see ESI), effect that has been predicted for the interior of a variety of charged polymeric systems from single chains, grafted polymer layers, star-like polyelectrolytes, to gels having different topologies[30,50–53]. This effect results in charge regulation, particularly from the diphenolic group of doxorubicin (see D2 in Fig. 1 with pKa 7.3), which protonates upon absorption. Inside the film, absorbed Doxo molecules are more positively charged, on average, than in the solution; this behavior is described in Fig. 7. At a fixed pH, the effect of lowering the solution salt concentrations is increasing the average charge of the absorbed molecules. In particular, the (apparent) pI of absorbed Doxo can increase several units in this way.

Next, we evaluate if doxorubicin can be released from the hydrogel when the material is in contact with polyamine solutions. Figure 8 shows Doxo absorption in the film from solutions that contain different concentrations of polyamines. As a reference, the graphs also include the absorption of doxorubicin from solutions containing no polyamines. We again consider physiological $[NaCl] = 100\,\text{mM}$ but extend the range of pH values to describe

View Article Online
DOI: 10.1039/D0SM00951B

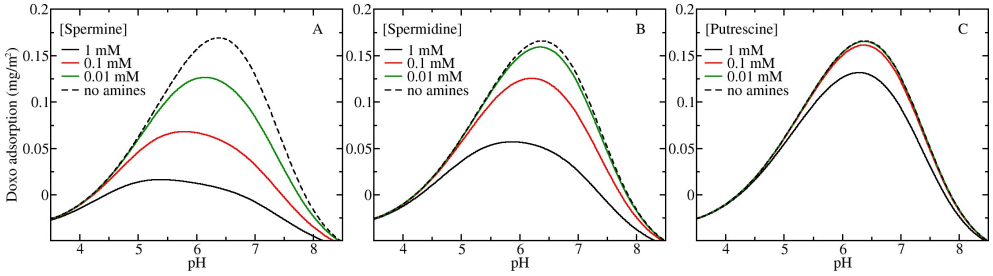

Fig. 8 Plot of the absorption of doxorubicin (see Eq. (2))as a function of pH for solutions containing spermine (A), spermidine (B) and putrescine (C). In each panel, the various solid-line curves correspond to solutions having different concentration of the polyamine, while the dashed-line curve corresponds to a solution without polyamines. All results correspond to 1 mM Doxo and 100 mM $NaCl$ solutions. (Theoretical predictions.)

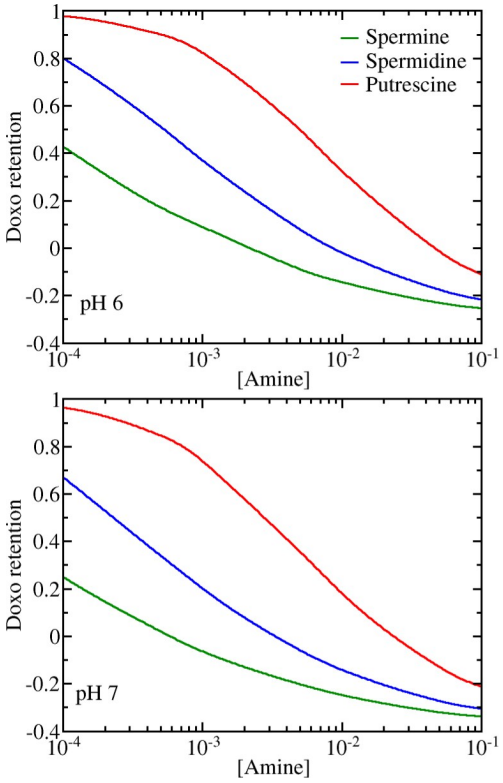

Fig. 9 Plot showing Doxo retention, Γ_{ret} (see Eq. (3)), as a function of the concentration of amines for solutions having 100 mM $NaCl$ and pH 6 (top panel) pH 7 (bottom panel). (Theoretical predictions.)

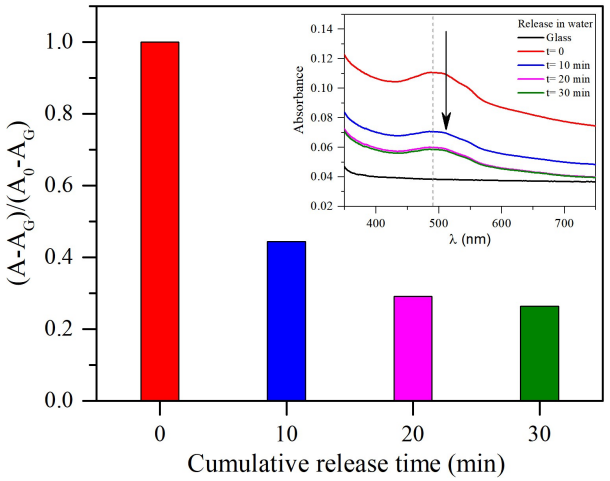

Fig. 10 Doxorubicin loading to and release from PMAA films in water, represented as the change in absorbance (at $\lambda = 490\,nm$) relative to the initial loading at different release times. Inset: Plot of the UV-Vis spectra of PMAA films after 24 h in contact with Doxo (red; $t = 0$). The various curves illustrate drug release after different release times to water. The black curve is included as a reference and corresponds to the signal of the bare glass support. A_G: Glass substrate absorbance; A_0: Fully loaded hydrogel absorbance.

conditions that might occur around acidic diseased tissue. Doxorubicin absorption is a nonmonotonic function of the solution pH, with a maximum between 6 and 7. This nonmonotonic behavior was to be expected since the net negative charge of the polymer is an increasing function of the solution pH (see Fig. 2), while the positive average charge of Doxo decreases until eventually turning negative at sufficiently high pH values (see Fig. 7).

Doxorubicin absorption decreases when polyamines are present in the solution (compare the different solid-line curves of Fig. 8 to the dashed-line curve in each panel), which results from polyamine capture as described in Fig. 5. This decrease in Doxo absorption with respect to solutions without the drug can be interpreted as a release from the film. Spermine being the strongest charged is the most efficient in preventing Doxo absorption (see panel A of Fig. 8).

To further quantify how the drug desorbs from the hydrogel film when amines are incorporated into the solution, we define the relative reduction in doxorubicin absorption:

$$\Gamma_{ret} = \frac{\Gamma_{\text{Doxo}}([Amine])}{\Gamma^0_{\text{Doxo}}} \qquad (3)$$

where Γ_{ret} is Doxo retention, $\Gamma_{\text{Doxo}}([Amine])$ is the doxorubicin absorption for amine solutions (see solid-line curves in Fig. 8), and $\Gamma^0_{\text{Doxo}} = \Gamma_{\text{Doxo}}([Amine] = 0)$ is that for solutions without polyamines (see Fig. 6 and dashed-line curves in Fig. 8).

Figure 9 shows Doxo retention in presence of each of the polyamines at physiological conditions as well as pH 6. If all the drug is kept inside the film for a polyamine solution, then $\Gamma_{ret} \approx 1$; while $\Gamma_{ret} \approx 0$ indicates that all the drug has been released. Negative values of Γ_{ret} can occur because $\Gamma_{\text{doxo}}([Amine])$, which is a bulk excess quantity, can take negative values, which indicates that under those conditions the amines prevent Doxo absorption in the film.

View Article Online
DOI: 10.1039/D0SM00951B

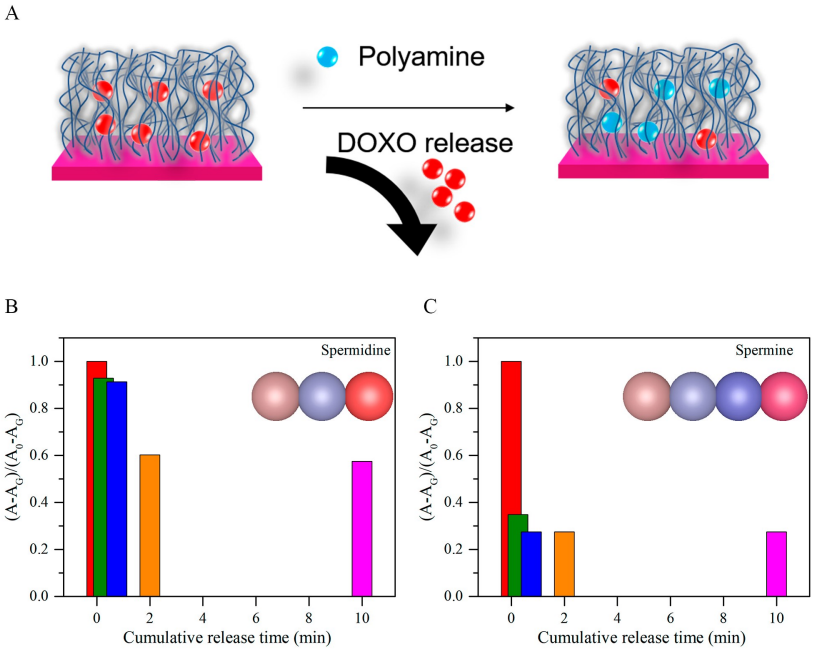

Fig. 11 Schematic representation of Doxo release by polyamine uptake (A). Doxorubicin loading to and release from PMAA films in spermine (B) and spermidine (C) solutions represented as the change in absorbance (at $\lambda = 490\,\text{nm}$) relative to the initial loading at different release times. A_G: Glass substrate absorbance; A_0: Fully loaded hydrogel absorbance.

Retention of doxorubicin within the hydrogel decreases as the concentration of polyamine rises. This is true for all the amines, and for pH 7 and 6 (see Figure 9). As aforementioned, spermine is the most efficient in promoting Doxo release from the hydrogel. At high amine concentrations, however, all polyamines can drive the release of significant quantities of doxorubicin.

3.2 UV-Vis Spectra

Doxorubicin loading in the hydrogel was characterized by UV-Vis experiments, analyzing the absorbance at $\lambda = 490\,\text{nm}$. To address the Doxo release after exposure to water, absorbance data was normalized accordingly, by subtracting the glass substrate absorbance (A_G) and then dividing by the absorbance of the fully loaded hydrogel (A_0), also with the A_G subtracted. Figure 10 shows the relative change in the absorbance after a given release time for a hydrogel previously loaded during 24 h. The inset shows the UV-Vis spectra after different release times in water. The experimental results at $t = 0$ (the red spectra shown in the inset of Fig. 10) evidence that the PMAA films incorporate doxorubicin within their polymeric network. The absorbance at $\lambda = 490\,\text{nm}$ for that spectra correspond to the red bar in the main figure. After sufficiently a long exposure time to water, the release from the films is only partial, demonstrating the affinity of the drug to the film. However, there is a clear and significant initial drug release within the first 10 minutes, behavior that is not observed in the subsequent release stages, where measurements collapse to the same spectra (see the inset of Figure 10).

Doxo release can be triggered by exposing the hydrogel film to polyamines, as depicted in Figure 11A. In order to evaluate this behavior, release experiments were performed using spermidine and spermine as model polyamines. Figure 11 shows the changes in relative absorbance for the PMAA films loaded with Doxo and its release in contact with spermidine (panel B) and spermine (panel C) solutions at different exposure times. Putrescine was not considered in the experiments due to the low absorption that presents in comparison with spermine and spermidine (see Fig. 5). The results show that the release of the drug in the presence of these polyamines is faster than in water, which supports the predictions of our theory and molecular modeling: PMAA hydrogels act as absorption platforms for polyamines, and such incorporation can trigger the release of a previously loaded drug.

Figure 11 B and C show that the release in the presence of spermine is faster than upon spermidine incorporation: after a 15 seconds exposure to spermine, there is no longer UV signal from Doxo, while a three times longer contact with spermidine is required to reach the same release stage. In addition, the magnitude of Doxo release using spermidine is less significant as opposed to the near complete release induced by spermine. These results indicate that the number of amino groups determines its retention in the hydrogel film, which is in line with the predictions from our molecular theory (see Fig. 9) and the work of Schimka *et al.* [48].

After the loading of polyamines and the concomitant Doxo release, the PMAA films were exposed to a fresh Doxo solution, to evaluate whether or not the absorption of polyamines would prevent doxorubicin re-absorption, as depicted in Fig. 12A. In other words, these experiments aim to answer if once released by polyamine absorption, doxorubicin would again be absorbed by

View Article Online
DOI: 10.1039/D0SM00951B

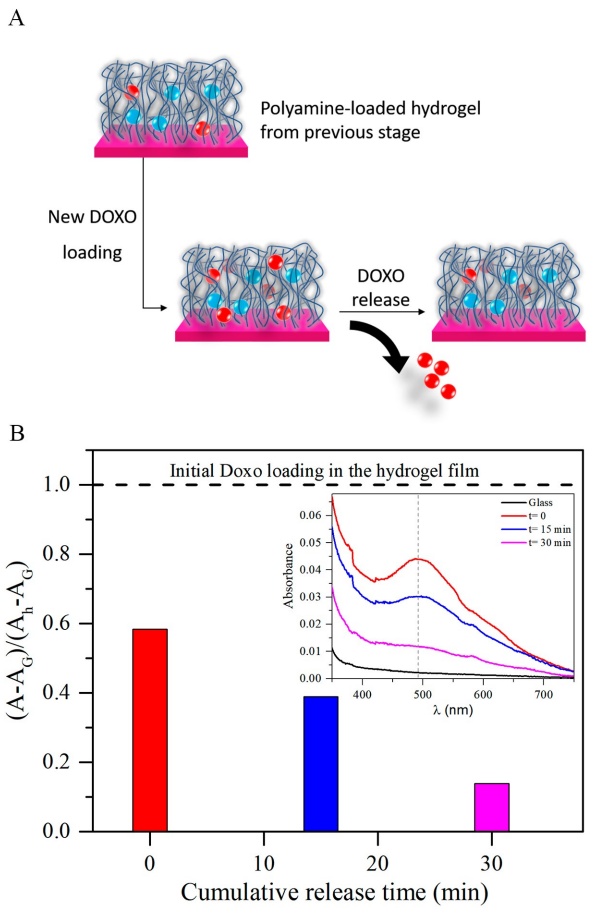

Fig. 12 (A) Schematic representation of Doxo re-loading/release after polyamine absorption. (B) The change in absorbance (at $\lambda = 490$ nm) relative to the initial Doxo loading in the hydrogel film (dashed line). A_G: Glass substrate absorbance; A_h: Absorbance for the initial Doxo loading in the hydrogel film (before polyamine absorption).

the hydrogel, decreasing its concentration in the medium. In line with the expected behavior, spermine retention by the hydrogel film significantly hinders Doxo re-absorption within the polymeric network (see Fig. S6 in the ESI). On the contrary, spermidine-loaded hydrogel films in contact with Doxo show the possibility to reload the drug, suggesting a different interaction intensity, depending on the polyamine. As shown in the panel B of Fig. 12, spermidine allows an initial reloading of Doxo into the film, but this loading is easily released to the media, as compared to the results of Fig. 10, where even after 1 hour of exposure to water, Doxo is not released. These results also highlight the stronger interaction of spermine (as compared to spermidine) with the polymeric network.

In summary, our experimental and theoretical results show the potentiality of hydrogel films based on PMAA to load therapeutic drugs, which was explored using Doxorubicin as model drug. While the hydrogel performs as a controlled release platform, the presence of high concentrations of polyamines in the surrounding media can trigger drug release by interacting with the polymeric network.

4 Conclusions

Polyamines are essential for cell metabolism as they are involved in different cellular processes, serving as nutrients for cell growth. In damaged cells that display uncontrolled growth, such as tumors, there is a surge in the need for nutrients, which causes a measurable excess in polyamine concentrations in the extracellular compartments. This increase in polyamine concentration plays a key role in the acceleration of tumor dissemination, and it can serve as an indicator of cancer cells. Anomalous polyamine concentrations can be the basis for therapies that target nutrient removal and metastasis prevention as well as used in means to evaluate the advance of a chemotherapy.

In this context, our goal in this work was to proof the following concept: can PMAA-based hydrogels be employed for developing biomaterials capable of both sequestering polyamines and delivering a therapeutic drug in response? We have developed a coarse grain molecular model to describe doxorubicin, putrescine, spermidine and spermine. Using this molecular model and a thermodynamic theory, our results provide insights into the absorption of polyamines and doxorubicin in PMAA hydrogel films.

These results predict the ability of PMAA hydrogels to capture increasing amounts of polyamines as the medium concentration increases at physiological salt conditions. This absorption increases with the number of amino groups; spermine displays the strongest preference for the hydrogel. This behavior results from the interaction between the positive charge of the amino groups and the deprotonated (negatively charged) MAA segments.

We have considered the loading of an anti-cancer drug as doxorubicin to the PMAA hydrogel. The optimal encapsulation conditions in the lab correspond to low salt concentration and pH between 6 to 7. This result is counterintuitive as doxorubicin isoelectric point is around neutral pH, which can be explained by protonation of the drug upon absorption within the lower pH medium inside the hydrogel.

When both doxorubicin and a polyamine are present in the solution in contact with the hydrogel, the polyamines significantly hinder drug absorption (as compared to solutions containing only doxorubicin). This effect is enhanced as the solution concentration of polyamines increases. The efficiency in excluding the drug from the film increases with the charge of the polyamine (*i.e.*, the number of amine groups); spermine is the most efficient of the three amines considered in achieving this response. As we have shown, this behavior can be interpreted as doxorubicin release upon polyamine capture.

PMAA films were synthesized *via* Atom Transfer Radical Polymerization and characterized at specific conditions to support our theoretical predictions. Doxorubicin absorption and release in water, spermidine and spermine solutions were studied using UV-Vis spectroscopy. These experimental results clearly support the proposed concept of doxorubicin encapsulation within these films and polyamine dependent drug release. Using the theoretical predictions of this work as a guideline, we are currently working on a systematic characterization of the experimental system.

In summary, our combined theoretical and experimental studies indicate that hydrogels based on poly(methacrylic acid) have

View Article Online
DOI: 10.1039/D0SM00951B

great potential to serve as the functional component in biomaterials that can capture polyamines and deliver a therapeutic drug in response.

Conflicts of interest

There are no conflicts to declare.

Acknowledgements

The authors thank financial support from CONICET and ANPCyT (PICT-2017-3513). NAPC acknowledges a fellowship from ANPCyT (PICT-2015-3425).

Notes and references

1 K. Igarashi and K. Kashiwagi, *Int. J. Biochem. Cell Biol.*, 2010, **42**, 39–51.
2 K. Soda, *Journal of Experimental & Clinical Cancer Research*, 2011, **30**, 95.
3 C. Moinard, L. Cynober and J.-P. de Bandt, *Clinical Nutrition*, 2005, **24**, 184–197.
4 R. A. Casero and P. M. Woster, *J. Med. Chem.*, 2009, **52**, 4551–4573.
5 A. E. Pegg and A. J. Michael, *Cell. Mol. Life Sci.*, 2010, **67**, 113–121.
6 C. W. Porter and R. J. Bergeron, *Science.*, 1983, **219**, 1083–1085.
7 D. H. Russell, *Clinical Chemistry*, 1977, **23**, 22–27.
8 D. H. Russell, C. C. Levy, S. C. Schimpff and I. A. Hawk, *Cancer Res.*, 1971, **31**, 1555–1558.
9 E. Agostinelli, M. Marques, R. Calheiros, F. Gil, G. Tempera, N. Viceconte, V. Battaglia, S. Grancara and A. Toninello, *Amino Acids*, 2010, **38**, 393–403.
10 S. L. Nowotarski, P. M. Woster and R. A. Casero, *Expert Rev. Mol. Med.*, 2013, **15**, 1–21.
11 M. H. Park and K. Igarashi, *Invit. Rev. Biomol Ther*, 2013, **21**, 1–9.
12 E. W. Gerner and F. L. Meyskens, *Nat. Rev. Cancer*, 2004, **4**, 781–792.
13 M. A. Jasnis, S. Klein, M. Monte, L. Davel, E. S. de Lustig and I. D. Algranati, *Cancer Letters*, 1994, **79**, 39–43.
14 M. Ikeda, T. Yoshii, T. Matsui, T. Tanida, H. Komatsu and I. Hamachi, *Journal of the American Chemical Society*, 2011, **133**, 1670–1673.
15 S. M. Aziz, M. N. Gillespie, P. A. Crooks, S. F. Tofiq, C. P. Tsuboi, J. W. Olson and M. P. Gosland, *Journal of Pharmacology and Experimental Therapeutics*, 1996, **278**, 185–192.
16 Y. Chen, R. S. Weeks, M. R. Burns, D. W. Boorman, A. Klein-Szanto and T. G. O'Brien, *International Journal of Cancer*, 2006, **118**, 2344–2349.
17 U. Bachrach, *Amino Acids*, 2004, **26**, 307–309.
18 Y. Wang, L. Guo, S. Dong, J. Cui and J. Hao, *Adv. Colloid Interface Sci.*, 2019, **266**, 1–20.
19 A. M. Lowman, M. Morishita, M. Kajita, T. Nagai and N. A. Peppas, *J. Pharm. Sci.*, 1999, **88**, 933–937.
20 X. Zhao and Z. Wang, *Colloids Surfaces B Biointerfaces*, 2019, **178**, 245–252.
21 M. Qindeel, N. Ahmed, F. Sabir, S. Khan and A. Ur-Rehman, *Drug Dev. Ind. Pharm.*, 2019, **0**, –000.
22 S. Li, L. Hu, D. Li, X. Wang, P. Zhang, J. Wang, G. Yan and R. Tang, *Int. J. Biol. Macromol.*, 2019, **129**, 477–487.
23 M. Kanamala, W. R. Wilson, M. Yang, B. D. Palmer and Z. Wu, *Biomaterials*, 2016, **85**, 152–167.
24 C. Panis, A. C. Herrera, V. J. Victorino, F. C. Campos, L. F. Freitas, T. De Rossi, A. N. Colado Simão, A. L. Cecchini and R. Cecchini, *Breast Cancer Res. Treat.*, 2012, **133**, 89–97.
25 M. J. Serpe, K. A. Yarmey, C. M. Nolan and L. A. Lyon, *Biomacromolecules*, 2005, **6**, 408–413.
26 C. Carvalho, M. Santos, S. Correia, R. Santos, S. Cardoso, P. Oliveira and P. Moreira, *Curr. Med. Chem.*, 2009, **16**, 3267–3285.
27 M. Kazempour, H. Namazi, A. Akbarzadeh and R. Kabiri, *Artif. Cells, Nanomedicine Biotechnol.*, 2019, **47**, 90–94.
28 A. Hagemann, J. M. Giussi and G. S. Longo, *Macromolecules*, 2018, **51**, 8205–8216.
29 G. S. Longo, N. A. Pérez-Chávez and I. Szleifer, *Curr. Opin. Colloid Interface Sci.*, 2019, **41**, 27–39.
30 R. Nap, P. Gong and I. Szleifer, *J. Polym. Sci. Part B Polym. Phys.*, 2006, **44**, 2638–2662.
31 P. Gong, J. Genzer and I. Szleifer, *Phys. Rev. Lett.*, 2007, **98**, 018302.
32 N. A. Pérez-Chávez, A. G. Albesa and G. S. Longo, *Langmuir*, 2018, **34**, 12560–12568.
33 R. A. Casero Jr and P. M. Woster, *Journal of Medicinal Chemistry*, 2009, **52**, 4551–4573.
34 *National Center for Biotechnology Information. PubChem Database. Doxorubicin, CID=3170*, `https://pubchem.ncbi.nlm.nih.gov/compound/Doxorubicin`.
35 B. A. Mann, C. Holm and K. Kremer, *J. Chem. Phys.*, 2005, **122**, 154903.
36 M. Quesada-Pérez, J. A. Maroto-Centeno and A. Martín-Molina, *Macromolecules*, 2012, **45**, 8872–8879.
37 P. Košovan, T. Richter and C. Holm, *Macromolecules*, 2015, **48**, 7698–7708.
38 C. Hofzumahaus, P. Hebbeker and S. Schneider, *Soft Matter*, 2018, **14**, 4087–4100.
39 B. Yameen, A. Kaltbeitzel, A. Langner, H. Duran, F. Müller, U. Gösele, O. Azzaroni and W. Knoll, *Journal of the American Chemical Society*, 2008, **130**, 13140–13144.
40 A. A. Brown, O. Azzaroni, L. M. Fidalgo and W. T. S. Huck, *Soft Matter*, 2009, **5**, 2738–2745.
41 P. Vaupel, F. Kallinowski and P. Okunieff, *Cancer Research*, 1989, **49**, 6449–6465.
42 I. F. Tannock and D. Rotin, *Cancer Res.*, 1989, **49**, 4373–4384.
43 N. Raghunand, X. He, R. van Sluis, B. Mahoney, B. Baggett, C. W. Taylor, G. Paine-Murrieta, D. Roe, Z. M. Bhujwalla and R. J. Gillies, *Br. J. Cancer*, 1999, **80**, 1005–1011.
44 E. K. Rofstad, B. Mathiesen, K. Kindem and K. Galappathi, *Cancer Research*, 2006, **66**, 6699–6707.
45 D. Schmaljohann, *Advanced Drug Delivery Reviews*, 2006, **58**,

View Article Online
DOI: 10.1039/D0SM00951B

1655–1670.

46 T. Koltai, *Onco. Targets. Ther.*, 2016, **9**, 6343–6360.

47 H. Sai, A. Erbas, A. Dannenhoffer, D. Huang, A. Weingarten, E. Siismets, K. Jang, K. Qu, L. C. Palmer, M. Olvera de la Cruz and S. I. Stupp, *J. Mater. Chem. A*, 2020, **8**, 158–168.

48 S. Schimka, N. Lomadze, M. Rabe, A. Kopyshev, M. Lehmann, R. Von Klitzing, A. M. Rumyantsev, E. Y. Kramarenko and S. Santer, *Phys. Chem. Chem. Phys.*, 2017, **19**, 108–117.

49 J. Zhang and N. A. Peppas, *Glass*, 2000, 102–107.

50 O. V. Borisov, E. B. Zhulina, F. A. M. Leermakers, M. Ballauff and A. H. E. Müller, in *Conformations and Solution Properties of Star-Branched Polyelectrolytes*, ed. A. H. E. Müller and O. Borisov, Springer Berlin Heidelberg, Berlin, Heidelberg, 2011, pp. 1–55.

51 G. S. Longo, M. Olvera de la Cruz and I. Szleifer, *Macromolecules*, 2011, **44**, 147–158.

52 A. A. Polotsky, F. A. Plamper and O. V. Borisov, *Macromolecules*, 2013, **46**, 8702–8709.

53 A. Murmiliuk, P. Košovan, M. Janata, K. Procházka, F. Uhlík and M. Štěpánek, *ACS Macro Lett.*, 2018, **7**, 1243–1247.

View Article Online
DOI: 10.1039/D0SM00951B

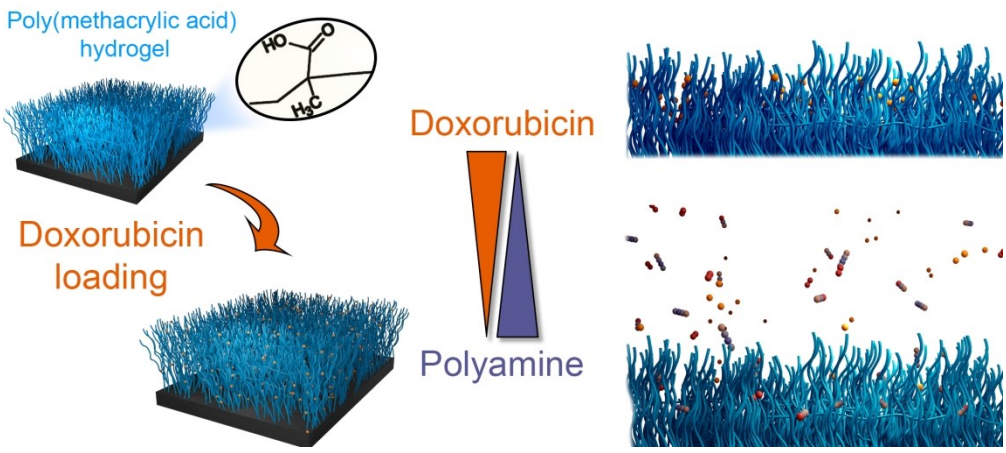

750x333mm (72 x 72 DPI)